

# NASA TECHNICAL MEMORANDUM

NASA TM X-71568

NASA TM X-71568

(NASA-TM-X-71568) FORMULATION OF A  
DISTORTION INDEX BASED ON PEAK COMPRESSOR  
PRESSURE RATIOS (NASA) 19 p HC \$3.00

N74-29306

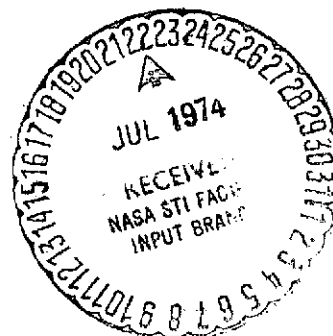
CSCL 20K

Unclas

G3/32 43364

## FORMULATION OF A DISTORTION INDEX BASED ON PEAK COMPRESSOR PRESSURE RATIOS

by James E. Calogeras and Paul L. Burstadt  
Lewis Research Center  
Cleveland, Ohio 44135



TECHNICAL PAPER presented at Eleventh National Conference on Environ-  
mental Effects on Aircraft and Propulsion Systems  
Trenton, New Jersey, May 21-23, 1974

FORMULATION OF A DISTORTION INDEX  
BASED ON PEAK COMPRESSOR PRESSURE RATIOS

James E. Calogeras and Paul L. Burstadt  
NASA-Lewis Research Center  
Cleveland, Ohio

AUTOBIOGRAPHIES

Mr. Calogeras obtained his B.S. degree in Aeronautical Engineering from the University of Detroit in 1964 and his M.S.E. degree in Aerospace Engineering from the University of Michigan in 1967. Since 1964, Mr. Calogeras has worked in the Inlet Systems Section of the Wind Tunnel and Flight Division. During the past six years, he has specialized in inlet-engine compatibility problems related to dynamic distortions produced by supersonic inlets.

Mr. Burstadt received his B.S.E. (1968) and M.S.E. (1973) degrees in Aerospace Engineering from the University of Michigan. Since joining NASA-Lewis in 1969, Mr. Burstadt has worked in the Inlet Systems Section of the Wind Tunnel and Flight Division. He has been primarily involved with experimental investigations of inlet-engine compatibility problems of airbreathing propulsion systems.

ABSTRACT

In order to effectively use a compressor face total-pressure distortion index as a measure of inlet-engine compatibility, a correlation of distortion amplitude with stall margin must be developed with minimal scatter. A recent analysis of data recorded in extensive distortion screen tests with the J85-GE-13 turbojet engine has resulted in a correlation based on compressor discharge pressure ratioed to the minimum pressure at the compressor face. Simply by determining compressor stall lines with a single hub radial distortion pattern, a single tip radial pattern, and with undistorted inflow, the overall compressor pressure ratio at stall for even the most complex distortion pattern was found to be predictable.

A simple compressor face distortion index has been formulated from these findings and has been applied to the data. This formulation represents a derivative of the parallel compressor theory. It is unique in its applicability to both radial and circumferential distortions, as well as combinations thereof.

## INTRODUCTION

In 1969, an experimental investigation was made in the NASA-Lewis Research Center Propulsion Systems Laboratory (PSL) Altitude Chamber to determine the effect of screen-induced total pressure distortion on the stall margin of a J85-GE-13 turbojet engine. Results of this test are reported in reference 1 and summarized in table I of this report. An empirical distortion index was formulated from these results and applied to a set of time-variant distortion data recorded in the Lewis Research Center 10- by 10-foot Supersonic Wind Tunnel with an axisymmetric mixed-compression inlet coupled to the identical J-85 engine (refs. 2 through 4). These results were in part inconclusive, and it is now known that the empirical distortion index derived from the 1969 screen test results was not applicable to many of the instantaneous distortion patterns that were produced in the supersonic inlet.

A motion picture made from a continuous series of instantaneous pressure contours best illustrates the problem of describing a distorted flow that can change drastically in a fraction of a second. Frames from the film were made by digitizing time-variant data from each of 30 compressor face dynamic total pressure probes, (cf. fig. 1), at a rate of 8000 samples per second. Contours were formed, utilizing a computer graphics program, from combined steady-state and time-variant pressures. A sample of these contours is presented in figure 2. Here each shaded region represents a range of total pressure recovery, with the darkest regions corresponding to the lowest recovery. The boundary between any two shaded regions is then a constant pressure contour. The map on the left was made from steady-state pressures. It represents almost a pure hub radial distortion. The one on the right is an instantaneous distortion contour plot. This pattern has a large circumferential distortion component. If it is understood that the steady-state contour results from a combination of perhaps hundreds of the instantaneous contours, the problem in developing a distortion index that adequately describes all these patterns becomes more evident.

In order to obtain results for a wider range of distortion patterns, a second screen-induced distortion test was run in the PSL facility in 1972. This test used two J-85 engines other than the one run in 1969. Results of this test are reported in reference 5 and summarized in table II of this report. The scatter of the correlation of distortion amplitude versus loss in compressor pressure ratio at stall grew. In 1973, a second attempt at correlating the entire 1969/1972 composite data set was initiated. This attempt was based on an approach called DIDENT (an acronym for "Distortion Identity"). Results to date are contained herein.

## RESULTS AND DISCUSSION

### Composite Data Set

A summary of the 1969/1972 composite data set is presented in figure 3. Parametric variations were made in the distortion intensity and the circumferential and/or radial extent of the spoiled area of many of these patterns. Compressor stalls were recorded at engine speeds ranging from 85- to 100-percent of rated engine speed. In all, 44 patterns and 176 stall points compose this data set. All of these points, with the exception of the full and partial midspan radial stall points, which had little or no effect on compressor performance or stability, were used in the DIDENT correlation.

### Parallel Compressor Concept

The basis of the DIDENT approach, presented in figure 4, is the parallel compressor concept suggested by Pearson and McKenzie in reference 6. This theory divides a compressor subjected to pressure distorted inflow into parallel compressors, each with an undistorted inflow of different total pressure. It is assumed that each compressor operates on the same undistorted compressor speed characteristic, that there are no crossflows between compressors, and that the compressors discharge to a constant and uniform static pressure.

In the case of the J-85 engine, compressor discharge total pressure is quite uniform, even with a severely distorted inlet flow. For this reason, average measured compressor discharge total pressure rather than static pressure was used in this parallel compressor theory model and the development of DIDENT. Further, the low pressure at the compressor face,  $(P_{\min, 60^\circ})_{2,r}$ , was defined as the lowest pressure, averaged over a  $60^\circ$  circumferential sector, in a ring immediately adjacent to either the hub or tip circumference and consisting of 20-percent of the compressor face flow area. In practice, averaging over  $60^\circ$  was only a consideration when the circumferential extent of the screen pattern was less than  $60^\circ$ . This averaging accounts for a minimum blade residence time in which the compressor may react in a steady-state manner, (cf. ref. 1). The concept of critical angle is somewhat analogous to an overall reduced frequency parameter, as pointed out by Williams and Yost in reference 7. Only the hub and tip instrumentation rings (cf. fig. 1) were used to define the minimum pressure since it was reasoned that stall would originate at either the root or tip sections of the blade. This reasoning has been somewhat substantiated by the negligible effect of full and partial midspan radial distortions (cf. refs. 1 and 5).

In its simplest form, the parallel compressor concept predicts compressor stall when the compressor pressure ratio of any of the parallel compressors intersects the undistorted stall line. The accuracy of this prediction for circumferential distortion patterns is shown in the next figure.

In figure 5, the peak compressor pressure ratio at stall  $\bar{P}_3 / (P_{\min, 60^\circ})_{2,r}$  is plotted as a function of corrected engine speed. The screen data represent all of the single and multiple per revolution circumferential distortions tested in the 1969 screen test. The solid curve is the undistorted stall line of the compressor.

The correlation here is very good, and it is about as good with the 1972 screen patterns of the same type. So apparently, the main premise of the parallel compressor concept holds very well for the J-85 engine, at least with circumferential distortions.

This same type correlation is presented in figure 6. In this case, the parallel compressor concept was applied to full and partial hub radial distortion patterns from the 1969 data set. The solid curve is faired through the data, and the broken line is the undistorted stall line of the compressor. At the higher corrected speeds, the faired curve falls somewhat above the undistorted stall line. This same result was found with the 1972 data of this type. It probably means that, once the distorted flow is inside the compressor, a spanwise flow redistribution takes place which attenuates the distortion. The interesting point of this figure is that, with reasonable accuracy, the solid line could be obtained by testing just one of these patterns.

In figure 7, peak compressor pressure ratios at stall are presented for full and partial tip radial patterns run in the 1969 test. Results are similar to the case of full and partial hub radial distortion but they fall on a different faired curve. Again, within reasonable accuracy, this curve could have been obtained by testing a single tip radial pattern.

A comparison of peak stall compressor pressure ratio fairings from the 1969 test is made with corresponding fairings from the 1972 test in figure 8. Both the hub and particularly the tip regions of the 1972 engine produced more pressure ratio at stall than did the 1969 engine. As might be expected, this resulted in about a 3-percent higher overall pressure ratio at stall for the undistorted (or full span circumferential) characteristic.

Unfortunately, these curves show that a tight correlation for a particular J-85 engine requires testing that particular serial number engine. But the results seem to indicate that the test would only require running a single hub radial, a single tip radial, and either a single circumferential or an undistorted stall line. This could represent a large reduction in the amount of screen testing needed in the development cycle of an engine.

#### Distortion Identity

In order to formulate a distortion index that would be useful for isolated inlet testing, the data from the curves of figure 8 was expressed in terms of compressor face total pressures and correlated with loss in stall compressor pressure ratio (LSPR). To accomplish this, an identifier function was first defined. This function ( $K_i$ ) is dependent on the basic distortion pattern, the serial number engine, and engine corrected speed. At a constant corrected speed, the identifier function  $K_i$  is simply the ratio of the regional to the undistorted stall pressure ratio, as shown in figure 8. Hence, for circumferential distortion,  $K_i = 1.0$ .

It was then possible to substitute the definition of the identifier function into the definition of LSPR to yield the distortion identity, DIDENT, as shown below:

Since

$$\text{LSPR} = \left\{ 1 - \frac{(\bar{P}_3/\bar{P}_2)_D}{(\bar{P}_3/\bar{P}_2)_U} \right\} N/\sqrt{\theta_2} = \text{const.}$$

and 
$$K_i = \left\{ \frac{[(P_{\min, 60^\circ})_{2,r}]/\bar{P}_2}{(\bar{P}_3/\bar{P}_2)_U} D \right\} N/\sqrt{\theta_2} = \text{const.} = f(\text{pattern, engine, } N/\sqrt{\theta_2})$$

then

$$\text{LSPR} = 1 - \frac{(P_{\min, 60^\circ})_{2,r}}{\bar{P}_2} K_i = \text{DI}$$

LSPR and  $K_i$  are both defined in terms of overall compressor pressure ratios at a constant corrected speed. Although many loss-in-stall-margin terms are defined at a constant corrected weight flow, the constant corrected speed definition was used in this case because it provided a better correlation.

With  $K_i = 1.0$  for circumferential distortions, DIDENT reduces to the same prediction offered in reference 7. In fact, figure 14 of reference 7 shows the good agreement between the circumferential distortion patterns run in the 1969 J-85 screen test with those from a series of rig tests run at Rolls-Royce and reported in reference 8.

The DIDENT correlation of the circumferential distortion patterns contained in the composite 1969/1972 J-85 data set is presented in figure 9. The solid line represents the distortion identity and the dashed lines represent a degree of scatter that was considered to be acceptable. The scatter of the open symbols about the theoretical line is due only to the original data scatter of the correlation presented in figure 5.

Figures 10 and 11, respectively, present the DIDENT correlation for most patterns contained in the 1969 and 1972 data sets. The full and partial midspan radial distortion patterns were omitted from these figures. The full and partial mid-span radial distortions were omitted because the present procedure of using hub and tip probes to define  $(P_{\min, 60^\circ})_{2,r}$  would generate small negative values of the distortion identity. This would in fact be quite accurate since the patterns did have measured values of LSPR that were zero or slightly negative. However, since the patterns had such a negligible effect on the stall line, they were ignored in this presentation. For the combined circumferential and partial radial distortion patterns and the instantaneous distortion pattern, values of  $K_i$  were determined from plots of the type shown in figures 5 through 7 included in reference 5.

Considering the simplicity of DIDENT, the correlation shown in these figures is very promising. Other than pattern numbers 1 and 10 in figure 11 (26.4% porosity screen), unacceptable scatter of most other stall points has been attributed to instrumentation inadequacies and interpolation errors.

## CONCLUDING REMARKS

The results presented demonstrate an approach to formulating a distortion descriptor (DIDENT) from a small number of classical distortion patterns. This descriptor uses a modified version of the parallel compressor concept to account for both radial and circumferential distortions. In this case the approach was applied to a turbojet engine with a single compression component. But there is nothing in the formulation or application of DIDENT that precludes its use for any type of turbine engine.

A summary of the present approach is as follows:

1. Determine critical angle  $\theta_{crit}$  (or overall reduced frequency parameter) for circumferential distortions.
2. Plot curves of  $\bar{P}_3 / (P_{min, \theta_{crit}})_{2,r}$  for circumferential, hub-radial and tip-radial distortion patterns as functions of corrected engine speed. Determine  $K_i$ .
3. Determine engine-to-engine variations of  $K_i$ . If necessary, determine the undistorted stall line for each serial number engine, together with a single hub-radial and single tip-radial stall line for each engine.
4. Evaluate the distortion identity (DIDENT). The present approach makes use of the fact that there was no total pressure distortion at the compressor discharge. If this were not the case,  $P_3$  would be replaced by  $p_3$  in the formulation of DIDENT.

Further work is planned to investigate the application of DIDENT to a multi-compressor turbine engine. A computer implementation of DIDENT is also planned that would be capable of evaluating a distortion pattern to determine whether the hub, tip, or circumferential identifier function,  $K_i$ , should be used. Such an implementation might use a series of radially averaged (i.e. rake average) pressures to identify circumferential distortions while retaining the use of hub and tip pressures to identify radial distortions. This implementation should be considered an integral part of the evaluation of DIDENT mentioned above in item 4.

## NOMENCLATURE

|       |   |  |
|-------|---|--|
| A     | area, $m^2 (ft^2)$  |  |
| DI    | distortion index, $1 - \frac{(P_{min, 60^\circ})_{2,r}}{\bar{P}_2} K_i$ |  |
| $K_i$ | identifier function, defined in "Results and Discussion"                |  |
| LSPR  | loss in stall compressor pressure ratio                                 | $\left\{ 1 - \frac{(\bar{P}_3/\bar{P}_2)_D}{(\bar{P}_3/\bar{P}_2)_U} \right\} \frac{N}{\sqrt{\theta_2}} = \text{const.}$ |

E-8305

E-8005

- M Mach number
- N engine speed, rpm
- N\* rated engine speed, 16,500 rpm
- $\frac{N \times 100}{N^* \sqrt{\theta_2}}$  corrected engine speed, percent
- P total pressure, N/m<sup>2</sup> (lbf/ft<sup>2</sup>)
- P static pressure, N/m<sup>2</sup> (lbf/ft<sup>2</sup>)
- T total temperature, K (°R)
- W engine airflow, Kg/sec (lbm/sec)
- $\frac{W \sqrt{\theta}}{S}$  corrected airflow, Kg/sec (lbm/sec)
- $\beta$  extent of pressure below average, deg.
- S local corrected total pressure, P/101325N/m<sup>2</sup> (P/2116lbf/ft<sup>2</sup>)
- $\theta$  local corrected total temperature, T/288.2K (T/518.7°R)
- $\theta_{crit}$  critical spoiled sector angle, degrees

Subscripts:

- D distorted inflow stall point
- sp spoiled or distorted
- U undistorted inflow stall point
- 1 mass flow measuring station
- 2 compressor face station
- 3 compressor discharge station
- min,60° lowest mean value in a 60° sector of station 2
- r inner or outer 20% area annulus of station 2

Superscripts:

spatial average

REFERENCES

1. Calogeras, J. E.; Mehalic, C. M.; and Burstadt, P. L.: Experimental Investigation of the Effect of Screen-Induced Total-Pressure Distortion on Turbojet Stall Margin. NASA TM X-2239, 1971.



2. Calogeras, J. E.; Burstadt, P. L.; and Coltrin, R. E.: Instantaneous and Dynamic Analysis of Inlet-Engine Compatibility. AIAA Paper 71-667, June, 1971.

3. Calogeras, J. E.: Instantaneous Distortion Investigation. NASA TM X-68189, 1972.

4. Burstadt, P. L.; and Calogeras, J. E.: Instantaneous Distortion in a Mach 2.5, 40-Percent-Internal-Contraction Inlet and its Effect on Turbojet Stall Margin. NASA TM X-3002, 1974.

5. Calogeras, J. E.; Johnsen, R. L.; and Burstadt, P. L.: The Effect of Screen-Induced Total-Pressure Distortion on Axial-Flow Compressor Stability. NASA TM X-3017, 1974.

6. Pearson, H.; and McKenzie, A. B.: Wakes in Axial Compressors. J. Roy. Aeronautics Society, Vol. 63, No. 583, July, 1959, pp. 415-416.

7. Williams, D. D.; and Yost, J. O.: Some Aspects of Inlet/Engine Flow Compatibility. Aeronautics Journal, Vol. 77, No. 753, September, 1973, pp. 483-492.

8. Reid, C.: The Response of Axial Flow Compressors to Intake Flow Distortion. ASME Paper 69-GT-29, March, 1969.

E-3005

TABLE I. - SCREEN PATTERNS

1969 Test Program

| Pattern | Type                           | Mesh            | Wire diameter, in. (cm) | Porosity, percent open | Circumferential extent, deg | Spotted area ratio, $A_{sp}/A_2$ | Percent corrected speed, $\frac{N}{N^*} \times 100$ | Screen pressure drop, $\frac{P_{min, 2}}{P_1}$ | Distortion amplitude, $\left(\frac{P_{max} - P_{min}}{P}\right)^2$ | Remarks  |
|---------|--------------------------------|-----------------|-------------------------|------------------------|-----------------------------|----------------------------------|---|--|--|--|
| 1       | Circumferential                | 7 $\frac{1}{2}$ | 0.032 (0.081)           | 57.4                   | 180                         | 0.50                             | 87.1<br>90.1<br>93.2<br>96.2<br>100.0               | 0.929<br>.914<br>.898<br>.874<br>.851          | 0.088<br>.085<br>.102<br>.125<br>.156                              | Stall point<br>↓                                       |
| 2       | Circumferential                | 8 $\frac{1}{2}$ | 0.035 (0.089)           | 49.8                   | 180                         | 0.50                             | 86.9<br>90.0<br>93.0<br>96.0<br>99.8                | 0.800<br>.882<br>.851<br>.834<br>.802          | 0.103<br>.122<br>.148<br>.176<br>.220                              | Stall point<br>↓                                       |
| 3       | Circumferential                | 9               | 0.041 (0.104)           | 39.7                   | 180                         | 0.50                             | 93.0<br>100.1                                       | 0.808<br>.745                                  | 0.196<br>.274  | Stall point<br>Stall point                             |
| 4       | Circumferential                | 7 $\frac{1}{2}$ | 0.032 (0.081)           | 57.4                   | 90                          | 0.25                             | 87.0<br>93.0<br>100.0                               | 0.932<br>.905<br>.864                          | 0.066<br>.091<br>.126  | Stall point<br>↓                                       |
| 5       | Circumferential                | 8 $\frac{1}{2}$ | 0.035 (0.089)           | 49.8                   | 90                          | 0.25                             | 87.0<br>89.9<br>92.9<br>95.9<br>99.7                | 0.918<br>.900<br>.885<br>.866<br>.840          | 0.080<br>.097<br>.112<br>.129<br>.159                              | Stall point<br>↓                                       |
| 6       | Circumferential                | 9               | 0.041 (0.104)           | 39.7                   | 90                          | 0.25                             | 92.9<br>100.0                                       | 0.849<br>.792                                  | 0.154<br>.215  | Stall point<br>Stall point                             |
| 7       | Circumferential                | 7 $\frac{1}{2}$ | 0.032 (0.081)           | 57.4                   | 60                          | 0.167                            | 86.9<br>89.9<br>92.9<br>96.0<br>99.9                | 0.937<br>.984<br>.912<br>.895<br>.870          | 0.058<br>.069<br>.080<br>.095<br>.113                              | Stall point<br>↓                                       |
| 8       | Circumferential                | 8 $\frac{1}{2}$ | 0.035 (0.089)           | 49.8                   | 60                          | 0.167                            | 86.7<br>89.9<br>92.8<br>96.1<br>99.7                | 0.922<br>.910<br>.894<br>.872<br>.848          | 0.070<br>.086<br>.097<br>.118<br>.138                              | Stall point<br>↓                                       |
| 9       | Circumferential                | 9               | 0.041 (0.104)           | 39.7                   | 60                          | 0.167                            | 87.3<br>92.9<br>99.8                                | 0.900<br>.863<br>.806                          | 0.094<br>.133<br>.189  | Stall point<br>↓                                       |
| 10      | Circumferential                | 8 $\frac{1}{2}$ | 0.035 (0.089)           | 49.8                   | 30                          | 0.083                            | 87.0<br>90.1<br>93.2<br>96.2<br>100.3               | 0.937<br>.923<br>.907<br>.890<br>.868          | 0.078<br>.095<br>.114<br>.135<br>.161                              | Stall point<br>↓                                       |
| 11      | Circumferential (dual sectors) | 8 $\frac{1}{2}$ | 0.035 (0.089)           | 49.8                   | 60                          | 0.333                            | 86.9<br>93.0<br>99.7                                | 0.913<br>.880<br>.822                          | 0.081<br>.110<br>.171  | Minimum $A_g$ ; no stall<br>Stall point<br>Stall point |
| 12      | Hub radial                     | 7 $\frac{1}{2}$ | 0.032 (0.081)           | 57.4                   | 360                         | 0.20                             | 87.0<br>92.9<br>99.9                                | 0.942<br>.920<br>.869                          | 0.055<br>.076<br>.126  | Stall point<br>↓                                       |
| 13      | Hub radial                     | 7 $\frac{1}{2}$ | 0.032 (0.081)           | 57.4                   | 360                         | 0.40                             | 86.9<br>92.9<br>99.9                                | 0.940<br>.913<br>.861                          | 0.055<br>.080<br>.130  | Stall point<br>↓                                       |

8005-E

TABLE I, - Concluded.

| Pattern | Type                                | Mesh                             | Wire diameter, in. (cm) | Porosity, percent open | Circumferential extent, deg | Spotted area ratio, $A_{sp}/A_3$ | Percent corrected speed, $\frac{N}{N\sqrt{\theta}} \times 100$ | Screen pressure drop, $\frac{P_{min.2}}{P_1}$ | Distortion amplitude, $\left(\frac{P_{max} - P_{min}}{P}\right)_2$ | Remarks                       |
|---------|-------------------------------------|----------------------------------|-------------------------|------------------------|-----------------------------|----------------------------------|--|---|--|-------------------------------|
| 14      | Hub radial                          | 9                                | 0.041 (0.104)           | 39.7                   | 360                         | 0.20                             | 87.1   | 0.908   | 0.087  | Stall point<br>↓              |
|         |                                     |                                  |                         |                        |                             |                                  | 90.2   | .895  | .100   |                               |
|         |                                     |                                  |                         |                        |                             |                                  | 93.0   | .876  | .118   |                               |
|         |                                     |                                  |                         |                        |                             |                                  | 96.0   | .852  | .151   |                               |
|         |                                     |                                  |                         |                        |                             |                                  | 99.9   | .810  | .189   |                               |
| 15      | Hub radial                          | 9                                | 0.041 (0.104)           | 39.7                   | 360                         | 0.40                             | 87.4   | 0.887   | 0.110  | Minimum $A_3$ ; no stall<br>↓ |
|         |                                     |                                  |                         |                        |                             |                                  | 90.2   | .875  | .123   |                               |
|         |                                     |                                  |                         |                        |                             |                                  | 93.5   | .853  | .146   |                               |
|         |                                     |                                  |                         |                        |                             |                                  | 96.0   | .830  | .172   |                               |
|         |                                     |                                  |                         |                        |                             |                                  | 100.1  | .777  | .233   |                               |
| 16      | Midspan radial                      | $7\frac{1}{2}$                   | 0.032 (0.081)           | 57.4                   | 360                         | 0.40                             | 86.9   | 0.934   | 0.055  | Stall point<br>↓              |
|         |                                     |                                  |                         |                        |                             |                                  | 89.8   | .922  | .065   |                               |
|         |                                     |                                  |                         |                        |                             |                                  | 92.9   | .908  | .078   |                               |
|         |                                     |                                  |                         |                        |                             |                                  | 95.9   | .882  | .099   |                               |
|         |                                     |                                  |                         |                        |                             |                                  | 100.0  | .858  | .126   |                               |
| 17      | Tip radial                          | $7\frac{1}{2}$                   | 0.032 (0.081)           | 57.4                   | 360                         | 0.15                             | 87.1   | 0.943   | 0.053  | Stall point<br>↓              |
|         |                                     |                                  |                         |                        |                             |                                  | 90.2   | .935  | .060   |                               |
|         |                                     |                                  |                         |                        |                             |                                  | 93.0   | .924  | .070   |                               |
|         |                                     |                                  |                         |                        |                             |                                  | 96.1   | .908  | .084   |                               |
|         |                                     |                                  |                         |                        |                             |                                  | 100.1  | .888  | .098   |                               |
| 18      | Tip radial                          | $7\frac{1}{2}$                   | 0.032 (0.081)           | 57.4                   | 360                         | 0.30                             | 92.9   | 0.906   | 0.068  | Stall point<br>↓              |
|         |                                     |                                  |                         |                        |                             |                                  | 95.8   | .887  | .107   |                               |
|         |                                     |                                  |                         |                        |                             |                                  | 98.8   | .865  | .127   |                               |
| 19      | Tip radial                          | $7\frac{1}{2}$                   | 0.032 (0.081)           | 57.4                   | 360                         | 0.60                             | 87.0   | 0.921   | 0.073  | Stall point<br>↓              |
|         |                                     |                                  |                         |                        |                             |                                  | 90.8   | .907  | .087   |                               |
|         |                                     |                                  |                         |                        |                             |                                  | 92.8   | .895  | .096   |                               |
|         |                                     |                                  |                         |                        |                             |                                  | 95.7   | .873  | .114   |                               |
|         |                                     |                                  |                         |                        |                             |                                  | 99.6   | .840  | .141   |                               |
| 20      | Tip radial                          | $8\frac{1}{2}$                   | 0.035 (0.089)           | 49.8                   | 360                         | 0.30                             | 92.9   | 0.883   | 0.115  | Stall point<br>Stall point    |
|         |                                     |                                  |                         |                        |                             |                                  | 99.9   | .837  | .170   |                               |
| 21      | Tip radial                          | $8\frac{1}{2}$                   | 0.035 (0.089)           | 49.8                   | 360                         | 0.60                             | 87.1   | 0.889   | 0.107  | Stall point<br>↓              |
|         |                                     |                                  |                         |                        |                             |                                  | 93.0   | .850  | .148   |                               |
|         |                                     |                                  |                         |                        |                             |                                  | 100.0  | .797  | .207   |                               |
| 22      | Graded tip radial                   | $8\frac{1}{2}$ (Outer ring)      | 0.035 (0.089)           | 49.8                   | 360                         | 0.30                             | 87.1   | 0.893   | 0.106  | Stall point<br>↓              |
|         |                                     |                                  |                         |                        |                             |                                  | 93.1   | .862  | .137   |                               |
|         |                                     | $7\frac{1}{2}$ (Inner ring)      | 0.032 (0.081)           | 57.4                   | 360                         | 0.30                             | 96.0   | .834  | .170   |                               |
|         |                                     |                                  |                         |                        |                             |                                  | 99.9   | .811  | .195   |                               |
| 23      | Hub radial sector                   | 9                                | 0.041 (0.104)           | 39.7                   | 120                         | 0.067                            | 87.1   | 0.912   | 0.080  | Stall point<br>↓              |
|         |                                     |                                  |                         |                        |                             |                                  | 90.0   | .897  | .095   |                               |
|         |                                     |                                  |                         |                        |                             |                                  | 93.0   | .881  | .108   |                               |
|         |                                     |                                  |                         |                        |                             |                                  | 96.1   | .857  | .132   |                               |
|         |                                     |                                  |                         |                        |                             |                                  | 100.0  | .825  | .161   |                               |
| 24      | Tip radial sector                   | 9                                | 0.041 (0.104)           | 39.7                   | 120                         | 0.133                            | 87.1   | 0.903   | 0.095  | Stall point<br>↓              |
|         |                                     |                                  |                         |                        |                             |                                  | 90.0   | .886  | .111   |                               |
|         |                                     |                                  |                         |                        |                             |                                  | 92.9   | .869  | .131   |                               |
|         |                                     |                                  |                         |                        |                             |                                  | 96.0   | .844  | .158   |                               |
|         |                                     |                                  |                         |                        |                             |                                  | 99.9   | .817  | .186   |                               |
| 25      | Combined radial and circumferential | $7\frac{1}{2}$ (Hub radial)      | 0.032 (0.081)           | 57.4                   | 270                         | 0.15                             | 87.0   | 0.818   | 0.076  | Stall point<br>↓              |
|         |                                     | $8\frac{1}{2}$ (Circumferential) | 0.035 (0.089)           | 49.8                   | 90                          | .25                              | 100.0  | .832  | .162   |                               |
| 26      | Combined radial and circumferential | $7\frac{1}{2}$ (Tip radial)      | 0.032 (0.081)           | 57.4                   | 270                         | 0.45                             | 87.0   | 0.920   | 0.084  | Stall point<br>↓              |
|         |                                     | $8\frac{1}{2}$ (Circumferential) | 0.032 (0.081)           | 57.4                   | 90                          | .25                              | 100.0  | .845  | .166   |                               |

E-8005

TABLE II. - SCREEN PATTERNS  
1972 Test Program

| Pattern | Type                    | Mesh number | Wire diameter, cm | Porosity, percent of open area | Circumferential extent, deg | Spotted-area ratio, $A_{SP}/A_2$ | Corrected engine speed, $\frac{N \times 100}{N \cdot \sqrt{S}}$ , percent of rated | Pressure ratio, $\left(\frac{P_{min, 60^\circ}}{P_1}\right)^{2.7}$ | Average inlet total pressure, $\bar{P}_1$ , N/m <sup>2</sup> | Pressure ratio, $\bar{P}_2/\bar{P}_1$ | Distortion, $\left[1 - \frac{P_{min, 60^\circ}}{\bar{P}} \sqrt{\frac{\beta_1}{\beta_2}}\right]^2$ | Engine | Remarks                                  |
|---------|-------------------------|-------------|-------------------|--------------------------------|-----------------------------|----------------------------------|--|--|--|---------------------------------------|---|--------|--|
| 1       | Circumferential         | 9           | 0.137             | 26.4                           | 180                         | 0.500                            | 88.7   | 0.795  | 86 571   | 0.883                                 | 0.0991  | A      | Stall point                              |
| 2       | Circumferential         | 9           | 0.137             | 26.4                           | 120                         | 0.333                            | 88.5   | 0.838  | 81 045   | 0.929                                 | 0.0772  | A      | Stall point                              |
|         |                         |             |                   |                                |                             |                                  | 92.8   | .776   | 87 610   | .902                                  | .1108   | A      | Stall point                              |
|         |                         |             |                   |                                |                             |                                  | 98.8   | .724   | 94 839   | .879                                  | .1400   | A      | Stall point                              |
| 3       | Circumferential         | 9           | 0.137             | 26.4                           | 60                          | 0.167                            | 88.4   | 0.878  | 69 620   | 0.961                                 | 0.0495  | A      | Stall point                              |
|         |                         |             |                   |                                |                             |                                  | 89.5   | .857   | 69 394   | .955                                  | .0583   |        |  |
|         |                         |             |                   |                                |                             |                                  | 92.8   | .834   | 69 268   | .947                                  | .0681   |        |  |
|         |                         |             |                   |                                |                             |                                  | 95.8   | .803   | 69 795   | .937                                  | .0823   |        |  |
|         |                         |             |                   |                                |                             |                                  | 98.9   | .771   | 69 863   | .927                                  | .0973   |        |  |
| 4       | Instantaneous           |             |                   |                                | ~180                        |                                  | 92.8   | 0.538  | 106 761  | 0.670                                 | 0.2015  | B      | Stall point (see RESULTS AND DISCUSSION) |
| 5       | Instantaneous           |             |                   |                                | ~120                        |                                  | 87.3   | 0.896  | 84 482   | 0.893                                 | 0.0478  | A      | T <sub>3</sub> limit - no stall          |
| 6       | Circumferential         | 9           | 0.081             | 50.6                           | 180                         | 0.500                            | 87.2   | 0.898  | 74 576   | 0.945                                 | 0.0428  | A      | Stall point                              |
|         |                         |             |                   |                                |                             |                                  | 92.8   | .860   | 77 003   | .924                                  | .0596   | A      |  |
|         |                         |             |                   |                                |                             |                                  | 98.5   | .818   | 80 047   | .899                                  | .0803   | A      |  |
|         |                         |             |                   |                                |                             |                                  | 87.2   | .901   | 74 762   | .946                                  | .0386   | B      |  |
|         |                         |             |                   |                                |                             |                                  | 93.2   | .865   | 77 974   | .921                                  | .0579   | B      |  |
| 98.5    | .822                    | 81 402      | .896              | .0769                          | B                           |                                  |  |  |  |                                       |   |        |  |
| 7       | Circumferential         | 9           | 0.081             | 50.6                           | 120                         | 0.333                            | 87.0   | 0.920  | 73 643   | 0.960                                 | 0.0342  | A      | Stall point                              |
|         |                         |             |                   |                                |                             |                                  | 92.9   | .887   | 75 990   | .944                                  | .0485   | A      | Stall point                              |
|         |                         |             |                   |                                |                             |                                  | 98.2   | .850   | 79 026   | .927                                  | .0667   | A      | Stall point                              |
| 8       | Circumferential         | 9           | 0.081             | 50.6                           | 60                          | 0.167                            | 86.9   | 0.927  | 69 582   | 0.971                                 | 0.0270  | A      | Stall point                              |
|         |                         |             |                   |                                |                             |                                  | 93.0   | .896   | 69 999   | .960                                  | .0375   | A      | Stall point                              |
|         |                         |             |                   |                                |                             |                                  | 98.1   | .855   | 69 431   | .946                                  | .0548   | A      | Stall point                              |
| 9       | Circumferential         | 9           | 0.081             | 50.6                           | 30                          | 0.083                            | 87.1   | 0.953  | 68 231   | 0.978                                 | 0.0144  | A      | Stall point                              |
|         |                         |             |                   |                                |                             |                                  | 93.0   | .923   | 68 532   | .968                                  | .0208   | A      | Stall point                              |
|         |                         |             |                   |                                |                             |                                  | 98.1   | .908   | 69 234   | .957                                  | .0284   | A      | Stall point                              |
| 10      | Hub radial              | 9           | 0.137             | 26.4                           | 360                         | 0.400                            | 99.5   | 0.712  | 81 311   | 0.842                                 | 0.1480  | A      | Stall point (engine failed)              |
|         |                         |             |                   |                                |                             |                                  | 87.2   | .833   | 74 722   | .908                                  | 0.0789  | B      | Stall point                              |
|         |                         |             |                   |                                |                             |                                  | 92.9   | .786   | 76 966   | .881                                  | 0.1025  |        |  |
|         |                         |             |                   |                                |                             |                                  | 96.1   | .795   | 78 853   | .863                                  | 0.1215  |        |  |
|         |                         |             |                   |                                |                             |                                  | 98.8   | .726   | 79 250   | .850                                  | 0.1408  |        |  |
| 11      | Circumferential (2/rev) | 9           | 0.081             | 50.6                           | 2/90                        | 0.500                            | 87.0   | 0.909  | 73 372   | 0.946                                 | 0.0234  | A      | Stall point                              |
|         |                         |             |                   |                                |                             |                                  | 88.8   | .900   | 76 486   | .943                                  | .0260   |        |  |
|         |                         |             |                   |                                |                             |                                  | 92.4   | .880   | 77 275   | .931                                  | .0321   |        |  |
|         |                         |             |                   |                                |                             |                                  | 98.0   | .838   | 80 884   | .906                                  | .0463   |        |  |
| 12      | Circumferential (2/rev) | 9           | 0.081             | 50.8                           | 2/45                        | 0.250                            | 86.9   | 0.938  | 74 212   | 0.987                                 | 0.0171  | A      | Stall point                              |
|         |                         |             |                   |                                |                             |                                  | 92.8   | .917   | 76 943   | .955                                  | .0221   | A      | Stall point                              |
|         |                         |             |                   |                                |                             |                                  | 98.9   | .871   | 81 619   | .933                                  | .0327   | A      | Stall point                              |
| 13      | Circumferential (2/rev) | 9           | 0.081             | 50.8                           | 2/30                        | 0.167                            | 87.3   | 0.955  | 73 742   | 0.972                                 | 0.0109  | B      | Stall point                              |
|         |                         |             |                   |                                |                             |                                  | 92.9   | .937   | 76 222   | .961                                  | .0154   | B      | Stall point                              |
|         |                         |             |                   |                                |                             |                                  | 98.5   | .907   | 79 558   | .945                                  | .0210   | B      | Stall point                              |
| 14      | Circumferential (4/rev) | 9           | 0.081             | 50.8                           | 4/30                        | 0.333                            | 86.9   | 0.943  | 73 153   | 0.962                                 | 0.0098  | B      | Stall point                              |
|         |                         |             |                   |                                |                             |                                  | 93.0   | .929   | 76 892   | .945                                  | .0085   | B      | Stall point                              |
|         |                         |             |                   |                                |                             |                                  | 98.6   | .887   | 81 554   | .922                                  | .0125   | B      | Stall point                              |

TABLE II. - Concluded.

|    |   |   |       |      |      |       |      |        |        |       |                     |             |                                 |
|----|---|---|-------|------|------|-------|------|--------|--------|-------|---------------------|-------------|---------------------------------|
| 15 | Combined radial and circumferential (2/rev) | 9 (Partial tip)<br>7½ (circumferential) | 0.081 | 50.6 | 2/90 | 0.100 | 87.1 | 0.922  | 71 932 | 0.976 | 0.0145              | B           | Stall point                     |
|    |   |   | .081  | 57.4 | 2/20 | .089  | 92.7 | .897   | 73 804 | .963  | .0204               | B           | Stall point                     |
|    |   |   |       |      |      |       | 98.8 | .844   | 79 057 | .945  | .0340               | B           | Stall point                     |
| 16 | Partial tip radial (4/rev)                  | 9                                       | 0.081 | 50.6 | 4/30 | 0.133 | 86.9 | 0.942  | 70 957 | 0.974 | 0.0052              | B           | Stall point                     |
|    |   |   |       |      |      |       | 92.9 | .925   | 71 030 | .966  | .0084               | B           | Stall point                     |
|    |   |   |       |      |      |       | 98.7 | .894   | 72 307 | .949  | .0120               | B           | T <sub>5</sub> limit - no stall |
| 17 | Partial hub radial                          | 9                                       | 0.104 | 39.7 | 120  | 0.113 | 86.9 | 0.908  | 68 433 | 0.974 | 0.0475              | B           | Stall point                     |
|    |   |   |       |      |      |       | 92.9 | .873   | 69 469 | .964  | .0661               | B           | Stall point                     |
|    |   |   |       |      |      |       | 98.6 | .832   | 69 920 | .954  | .0887               | B           | Stall point                     |
| 18 | Partial hub radial                          | 9                                       | 0.104 | 39.7 | 120  | 0.087 | 88.9 | 0.905  | 70 294 | 0.970 | 0.0427              | B           | Stall point                     |
|    |   |   |       |      |      |       | 92.9 | .869   | 71 452 | .959  | .0596               | B           | Stall point                     |
|    |   |   |       |      |      |       | 98.4 | .824   | 72 973 | .946  | .0845               | B           | Stall point                     |
| 19 | Partial hub radial                          | 9                                       | 0.104 | 39.7 | 60   | 0.057 | 86.8 | 0.909  | 68 209 | 0.976 | 0.0368              | B           | Stall point                     |
|    |   |   |       |      |      |       | 92.8 | .874   | 68 793 | .967  | .0509               | B           | Stall point                     |
|    |   |   |       |      |      |       | 98.5 | .830   | 68 603 | .956  | .0710               | B           | Stall point                     |
| 21 | Partial hub radial                          | 9                                       | 0.104 | 30.7 | 30   | 0.028 | 86.7 | 0.947  | 68 885 | 0.979 | 0.0174              | B           | Stall point                     |
|    |   |   |       |      |      |       | 92.5 | .926   | 68 943 | .971  | .0242               | B           | Stall point                     |
|    |   |   |       |      |      |       | 97.7 | .903   | 69 163 | .982  | .0323               | B           | Stall point                     |
| 23 | Partial tip radial                          | 9                                       | 0.104 | 39.7 | 120  | 0.133 | 86.9 | 0.902  | 71 020 | 0.989 | 0.0377              | B           | Stall point                     |
|    |   |   |       |      |      |       | 92.9 | .869   | 72 542 | .958  | .0636               | B           | Stall point                     |
|    |   |   |       |      |      |       | 98.5 | .822   | 74 568 | .943  | .0771               | B           | Stall point                     |
| 24 | Partial tip radial                          | 9                                       | 0.104 | 39.7 | 120  | 0.067 | 87.2 | 0.917  | 68 808 | 0.977 | 0.0311              | B           | Stall point                     |
|    |   |   |       |      |      |       | 92.9 | .884   | -----  | ----- | .0443               | B           | Data recording no good          |
|    |   |   |       |      |      |       | 98.3 | .854   | 68 874 | .956  | .0666               | B           | Stall point                     |
| 25 | Partial tip radial                          | 9                                       | 0.104 | 39.7 | 60   | 0.087 | 87.0 | 0.911  | 69 505 | 0.976 | 0.0294              | B           | Stall point                     |
|    |   |   |       |      |      |       | 92.9 | -----  | 69 763 | .982  | .0510               | B           | Stall point                     |
|    |   |   |       |      |      |       | 98.7 | .831   | 69 633 | .953  | .0598               | B           | Stall point                     |
| 29 | Mid-span partial radial                     | 9                                       | 0.104 | 39.7 | 120  | 0.087 | 86.6 | 0.914  | 74 081 | 0.973 | 0.0432              | B           | Stall point                     |
|    |   |   |       |      |      |       | 92.6 | .885   | 76 794 | .984  | .0583               | B           | Stall point                     |
|    |   |   |       |      |      |       | 97.8 | .840   | 80 766 | .948  | .0811               | B           | Stall point                     |
| 30 | Combined patterns 10 and 23                 | 9 (Hub radial)                          | 0.137 | 26.4 | 360  | 0.400 | 87.0 | 0.933  | 74 218 | 0.898 | 0.0620              | B           | Stall point                     |
|    |   | 9 (Partial tip radial)                  | .104  | 39.7 | 120  | .133  | 92.8 | .911   | 76 990 | .861  | .0850               | B           | Stall point                     |
|    |   |   |       |      |      | 98.4  | .881 | 80 824 | .816   | .1195 | B                   | Stall point |                                 |
| 31 | Hub radial                                  | 9                                       | 0.104 | 39.7 | 360  | 0.400 | 86.9 | 0.892  | 71 506 | 0.939 | <sup>a</sup> 0.0487 | B           | T <sub>5</sub> limit - no stall |
|    |   |   |       |      |      |       | 92.8 | .857   | 72 570 | .922  | <sup>a</sup> .0688  | B           | Stall point                     |
|    |   |   |       |      |      |       | 98.2 | .795   | 73 513 | .889  | <sup>a</sup> .1026  | B           | Stall point                     |
| 32 | Combined hub radial and partial tip radial  | 9 (Hub radial)                          | 0.104 | 39.7 | 360  | 0.400 | 87.0 | 0.871  | 77 808 | 0.910 | 0.0578              | B           | Stall point                     |
|    |   | 9 (Partial tip radial)                  | .104  | 39.7 | 120  | .200  | 92.8 | .838   | 80 664 | .885  | .0744               | B           | Stall point                     |
|    |   |   |       |      |      | 98.7  | .766 | 80 435 | .830   | .1179 | B                   | Stall point |                                 |
| 33 | Combined patterns 23 and 31                 | 9 (Hub radial)                          | 0.104 | 39.7 | 360  | 0.400 | 86.7 | 0.883  | 70 829 | 0.925 | 0.0516              | B           | Stall point                     |
|    |   | 9 (Partial tip radial)                  | .104  | 39.7 | 120  | .133  | 92.6 | .845   | 72 827 | .900  | .0704               | B           | Stall point                     |
|    |   |   |       |      |      | 97.9  | .777 | 76 335 | .868   | .1077 | B                   | Stall point |                                 |

<sup>a</sup>DPR distortion definition (appendix B).

E-8005

### STEADY-STATE AND DYNAMIC PRESSURE INSTRUMENTATION

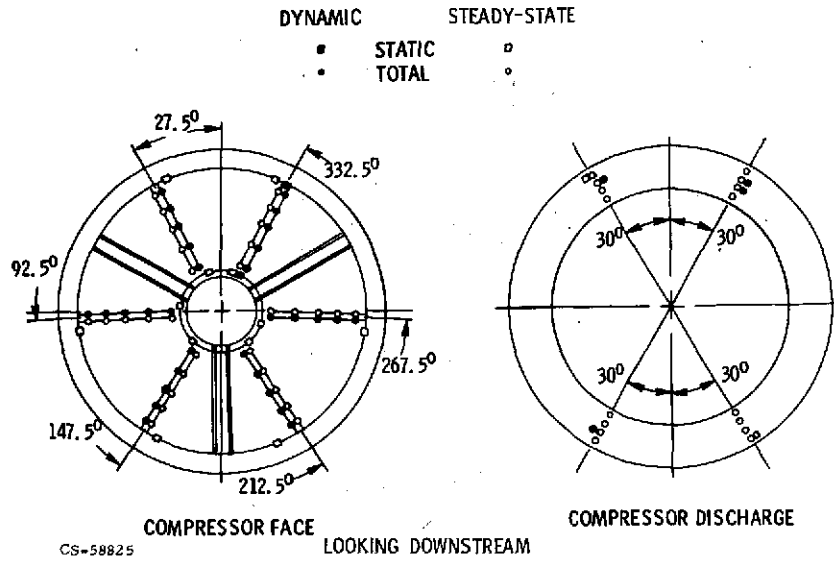


Figure 1.

### DISTORTION CONTOURS

$\alpha = 0^\circ$  STALL POINT

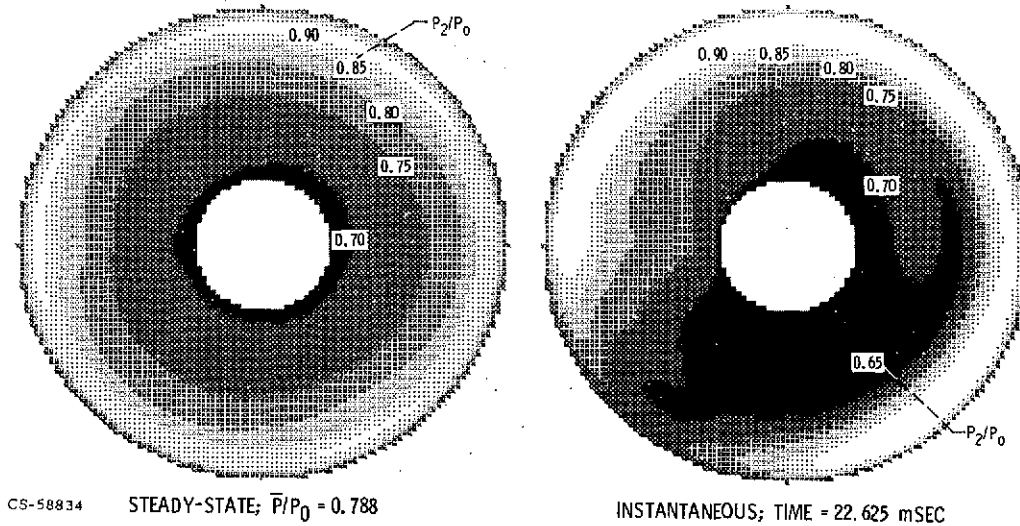


Figure 2.

COMPOSITE DATA SET  
J85-GE-13 SCREEN TESTS





| PATTERNS,<br>TYPE |  | TOTALS   |        |
|-------------------|---|----------|--------|
|                   |   | PATTERNS | STALLS |
| CIRCUMFERENTIAL   |   | 18       | 76     |
| RADIAL            |  | 12       | 49     |
| PARTIAL RADIAL    |  | 8        | 33     |
| COMBINED          |  | 6        | 18     |

Figure 3.

CS-70112

PARALLEL COMPRESSOR CONCEPT

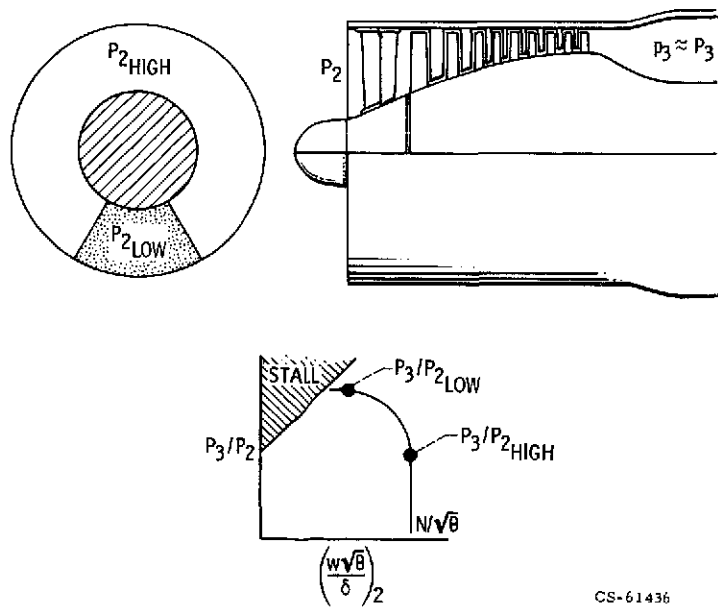


Figure 4.

CS-61436

PEAK STALL PRESSURE RATIOS  
CIRCUMFERENTIAL DISTORTION

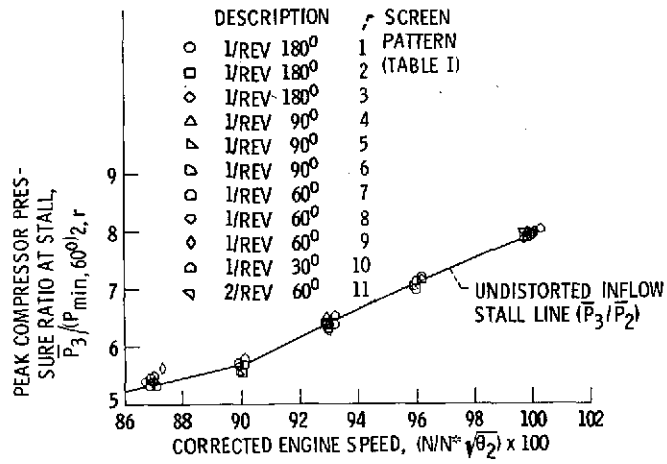


Figure 5.

CS-70110

PEAK STALL PRESSURE RATIOS  
FULL & PARTIAL HUB RADIAL DISTORTION

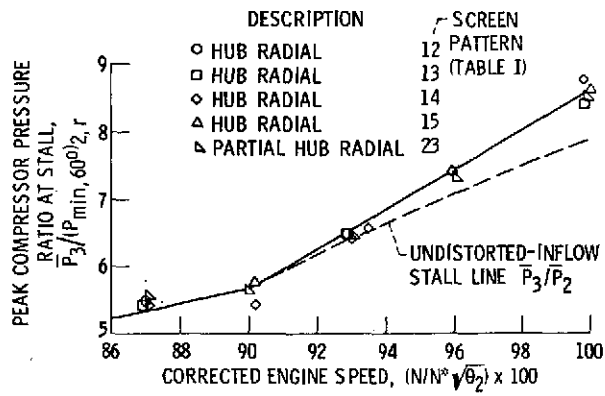


Figure 6.

CS-70107



PEAK STALL PRESSURE RATIOS  
FULL & PARTIAL TIP RADIAL DISTORTION

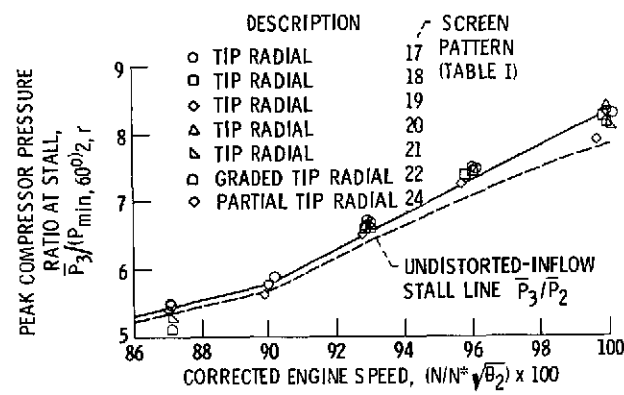


Figure 7. CS-70106

SUMMARY OF PEAK STALL PRESSURE RATIOS

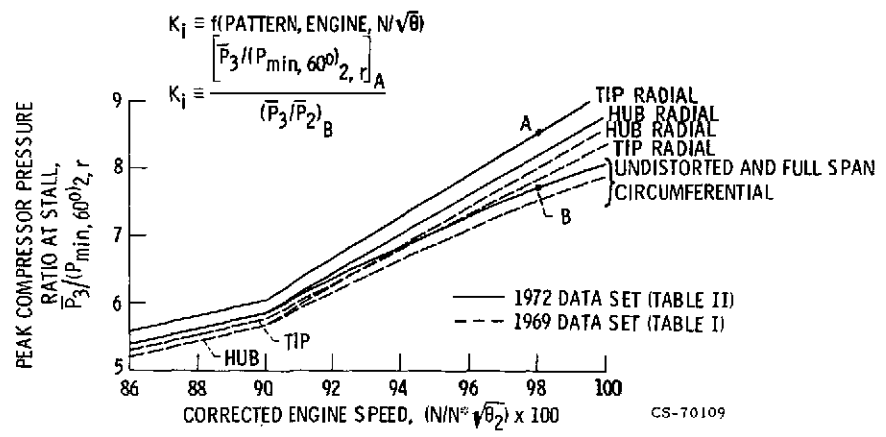


Figure 8.

CORRELATION OF CIRCUMFERENTIAL DISTORTION DATA

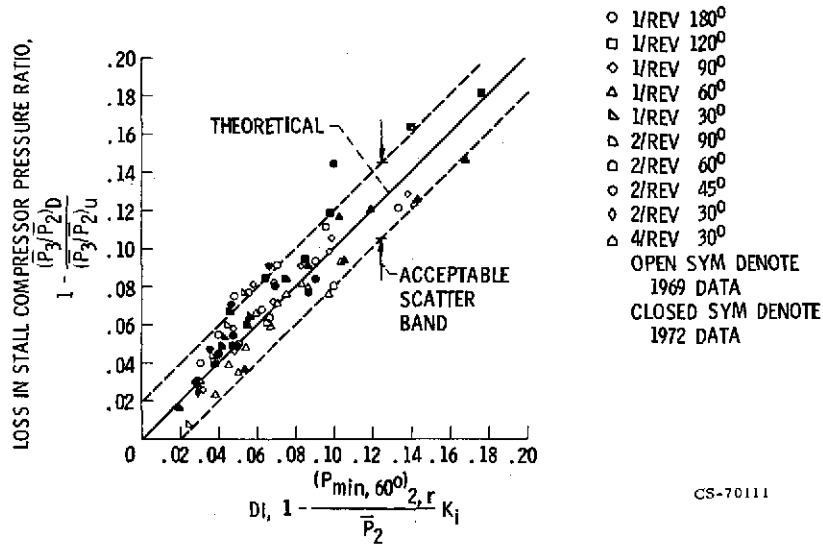


Figure 9.

CORRELATION OF 1969 DISTORTION DATA SET

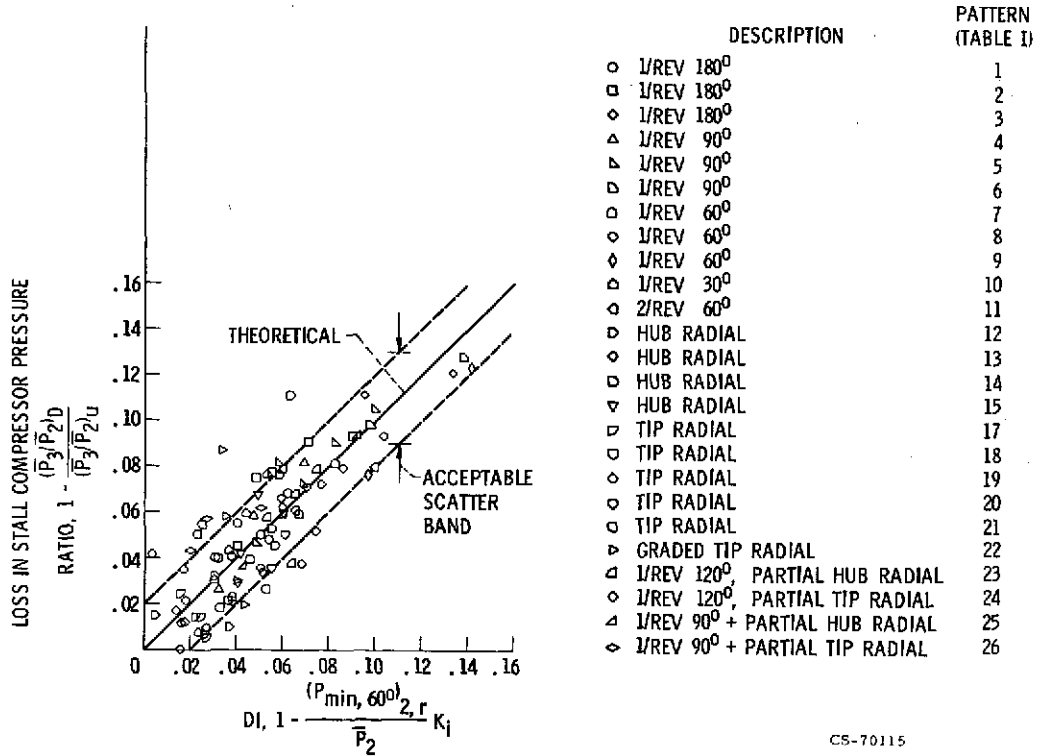
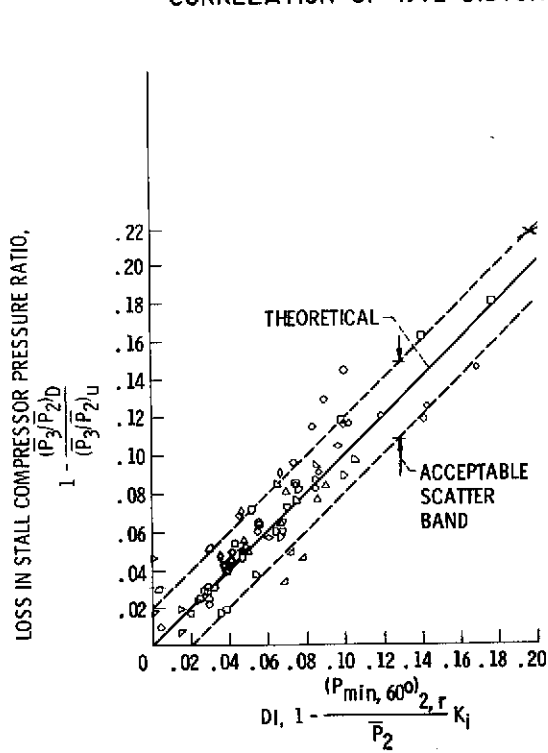


Figure 10.

CORRELATION OF 1972 DISTORTION DATA SET



| DESCRIPTION                      | PATTERN (TABLE II) |
|----------------------------------|--------------------|
| ○ 1/REV 180°                     | 1                  |
| □ 1/REV 120°                     | 2                  |
| ◇ 1/REV 60°                      | 3                  |
| △ 1/REV 180°                     | 6                  |
| ▽ 1/REV 120°                     | 7                  |
| ◊ 1/REV 60°                      | 8                  |
| ○ 1/REV 30°                      | 9                  |
| ○ HUB RADIAL                     | 10                 |
| ◇ 2/REV 90°                      | 11                 |
| ◇ 2/REV 45°                      | 12                 |
| △ 2/REV 30°                      | 13                 |
| △ 4/REV 30°                      | 14                 |
| ▷ 2/REV 20° + PARTIAL TIP RADIAL | 15                 |
| ▽ 4/REV 30°, PARTIAL TIP RADIAL  | 16                 |
| ▽ 1/REV 120°, PARTIAL HUB RADIAL | 17                 |
| ○ 1/REV 120°, PARTIAL HUB RADIAL | 18                 |
| △ 1/REV 60°, PARTIAL HUB RADIAL  | 19                 |
| △ 1/REV 30°, PARTIAL HUB RADIAL  | 21                 |
| ○ 1/REV 120°, PARTIAL TIP RADIAL | 23                 |
| ○ 1/REV 120°, PARTIAL TIP RADIAL | 24                 |
| ○ 1/REV 60°, PARTIAL TIP RADIAL  | 25                 |
| ○ HUB RADIAL                     | 31                 |
| ○ COMBINED HUB RADIAL &          | 30                 |
| ○ 1/REV 120°, PARTIAL TIP RADIAL | 32                 |
| ○ 1/REV 120°, PARTIAL TIP RADIAL | 33                 |
| × INSTANTANEOUS                  | 4                  |

CS-70114

Figure 11.

E-8005